Connecting Local Yield Stresses with Plastic Activity in Amorphous Solids

Sylvain Patinet, Damien Vandembroucq, and Michael L. Falk

Phys. Rev. Lett. **117**, 045501 — Published 20 July 2016

DOI: 10.1103/PhysRevLett.117.045501

Connecting local yield stresses with plastic activity in amorphous solids

Sylvain Patinet,[1,*] Damien Vandembroucq,[1] and Michael L. Falk[2]

[1] *Laboratoire de Physique et Mécanique des Milieux Hétèrogènes (PMMH), UMR CNRS 7636 ; PSL - ESPCI, 10 rue Vauquelin, 75005 Paris, France; Sorbonne Université - UPMC, Univ. Paris 06; Sorbonne Paris Cité - UDD, Univ. Paris 07*

[2] *Departments of Materials Science and Engineering, Mechanical Engineering, and Physics and Astronomy, Johns Hopkins University, Baltimore, MD 21218 USA*

(Dated: June 21, 2016)

In model amorphous solids produced via differing quench protocols, a strong correlation is established between local yield stress measured by direct local probing of shear stress thresholds and the plastic rearrangements observed during remote loading in shear. This purely local measure shows a higher predictive power for identifying sites of plastic activity when compared with more conventional structural properties. Most importantly, the sites of low local yield stress thus defined are shown to be persistent, remaining predictive of deformation events even after fifty or more such plastic rearrangements. This direct and non-perturbative approach gives access to relevant transition pathways that control the stability of amorphous solids. Our results reinforce the relevance of modeling plasticity in amorphous solids based on a gradually evolving population of discrete and local zones pre-existing in the structure.

Unlike in crystalline materials, the modeling of plasticity in amorphous materials is still limited to qualitative or phenomenological approaches. Indeed, the absence of clearly identified topological defects, such as dislocations, excludes systematic characterization of the mechanisms occurring at the smallest scales [1]. It has long been hypothesized that, at the atomic scale, the plasticity of amorphous materials manifests as local rearrangements, exhibiting characteristic quadrupolar stress signatures [2–7] leading to a redistribution of elastic stresses in the system [5, 8, 9]. By analogy with dislocations, it therefore appears natural to try to describe the plastic flow from the dynamics of some localized "defects". This vision of plasticity has led to the concept of Shear Transformation Zones (STZ) [3], meaning zones (i) that pre-exist within the material prior to the loading, (ii) rearranging under shear, (iii) resulting in plastic deformation, and (iv) persist during deformation until the activation of other nearby zones results in the local reshuffling of atoms. Starting from these building blocks, mean-field theories [3, 10–12] and lattice-based models [13–15] have been developed to model amorphous plasticity. Many of these studies have sought to connect local structural properties with effective plastic activity in order to physically ground these models.

However, despite many attempts to link structure and plasticity, most of the structural indicators studied, such as free volume, elastic moduli, local stresses, and local favorable structures, have shown a relatively low correlation with the plastic activity and are critically material-dependent [1, 16–18]. So far, the most promising physically-based method to predict the relaxation locations via atomistic computations involves identifying "soft spots" based on the soft vibrational modes [17–23]. This perturbative method is substantially predictive only close to instabilities, however, and relies on a system-dependent determination of the number of modes considered. Furthermore, it only gives access to a "mobility field" and not more physically relevant quantities such as stress thresholds or energy barriers. Prior applications of non-perturbative methods to harvest activation energies between configurational states in glasses have revealed interesting trends, but have not proven predictive of the locations of future plastic events [24–26].

The lack of accurate and physically well-grounded local characterization methods has led some to question the relevance of modeling plastic deformation in the framework of pre-existing zones such as STZs [27, 28]. The aim of this letter is to propose a measure of the local plastic susceptibility from atomistic simulations. We believe that the success of the local yield stress measure described here clearly demonstrates the relevance of the STZ picture, and lays the groundwork to place such approaches on a firm quantitative foundation. We perform series of local shear tests over a range of different orientations on a two-dimensional model glass. We then systematically compute the minimum shear stresses that trigger irreversible plastic rearrangements. This straightforward simulation technique allows us to access the local stress thresholds and predicts not only the most plastically susceptible zone along an orientation, but also characterizes the population of zones for a given material state. We demonstrate a strong correlation between a broad population of low local thresholds and plastic activity observed during remote loading. The correlation obtained shows a higher degree of predictability when compared to previously studied structural indicators. Furthermore, we show that these zones are long lived and survive many plastic rearrangements. All of these results support the relevance of a description of plastic deformation based on

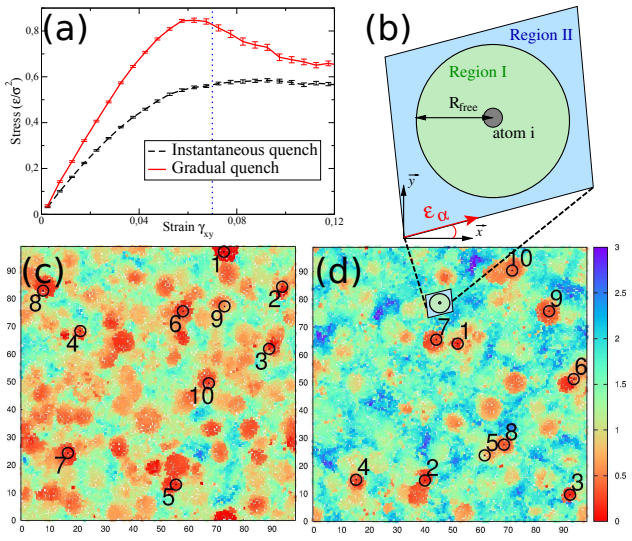

FIG. 1. a) Average stress-strain curves for instantaneous (dashed lines) and gradual (continuous lines) quenches. The vertical line is located at $\gamma_{xy} = 0.07$. b) Schematic drawing of the local yield stress computation around an atom i: region I is fully relaxed while region II is forced to deform following an affine shear deformation in the α direction. Local yield stress maps τ_y (see Eq.(1)) defined for each atom for an instantaneously (c) and a gradually (d) quenched system. The first 10 plastic event locations are shown as open black symbols numbered by order of appearance during remote shear loading.

the dynamic of discrete plastic zones.

Simulation methods - Atomistic simulations [29] are performed to investigate the mechanical properties of a two-dimensional binary glass forming system [30, 31] previously employed in [3, 32, 33]. Fifty glass samples containing 10^4 atoms are synthesized using the same interatomic potential, composition, density and quench protocols as in [33]. The two types of atoms interact via standard Lennard-Jones interatomic potentials. All units will be expressed in terms of the mass m of the atoms, which are equal, as well as ϵ and σ, the parameters describing the energy and length scale, respectively, of the interspecies interaction. The characteristic time is $t_0 = \sigma\sqrt{m/\epsilon}$. The glass transition temperature T_g of this system is known to be located approximately at $T_g = 0.325\epsilon/k$, where k is the Boltzmann constant.

Glass samples are obtained by reducing the temperature from a liquid state, equilibrated at $1.08T_g$. In order to highlight the links between the processing of glasses, their microstructures and their mechanical properties, two different quench rates are considered: one infinitely rapid and another as slow as possible using molecular dynamics simulation. The first one is derived directly from the high temperature liquid while the temperature in the more deeply quenched system is reduced continuously to a low-temperature solid state equal to $0.092T_g$ over a period of $10^6 t_0$ using a Nose-Hoover thermostat [34, 35]. In both cases, a static relaxation via a conjugate gradient method is applied to bring the system to mechanical equilibrium at zero temperature.

As reported in Fig. 1a, the glasses are deformed in simple shear with an Athermal Quasi Static method (AQS) [5–7, 16, 27, 36]. This incremental method consists in applying a series of deformation steps, $\Delta\gamma_{xy} = 10^{-5}$, by moving the atom positions to follow an affine displacement field. After each deformation increment, the system is relaxed to its mechanical equilibrium. The observed response is typical for amorphous materials and is characterized by reversible elastic branches interspersed by plastic events [37]. The displacement fields induced by the successive plastic events are calculated from the difference between the position of the atoms after and just before each instability. The strain tensor ϵ_{ij} is then evaluated from the displacement field following the method developed in Ref. [38]. The position of a plastic event is defined as the position of the atom i_{max} having undergone the maximum shear deformation. This approach allows us to obtain the successive positions of the localized plastic events during deformation from the quenched state as reported in Fig. 1 [39].

Probing local yield stress - We now propose a characterization of the plastic properties of the model glass at the local scale. In the present study, a length scale equal to 5σ is chosen to perform this investigation [39]. We extend a method proposed by Sollich [40] to compute local yield stresses. This consists of constraining the atoms outside a circular region of radius $R_{free} = 5\sigma$ to deform in a purely affine manner to locally probe the mechanical response within the embedded region. The same AQS method is used as in the shearing of the entire sample but only the atoms within the region are relaxed and can deform non-affinely. Plastic rearrangements are thus forced to occur within this region and the local yield stress can be identified. An important feature of our study is an assessment of the orientational nature of the plastic rearrangements [3]. Due to the randomness of the amorphous structure, the yield stress may not be the same for all orientations of the imposed shear. Sollich's approach is thus extended to shear the system in several orientations α as depicted in Fig. 1b. The local shear stress [41] at the onset of the instability $\tau^{inst}(\alpha)$ is recorded for each direction of shear. The shear stress threshold along the loading direction is then deduced as the difference $\tau^c(\alpha) = \tau^{inst}(\alpha) - \tau^0(\alpha)$ where $\tau^0(\alpha)$ is the initial local shear stress state of the region within the as-quenched glass. The stress $\tau^c(\alpha)$ thus corresponds to the mean shear stress along α that has to be added on the atoms in the region (or, equivalently, the change in the mean stress imposed on the boundary of it) to trigger a rearrangement. This operation is performed for orientations from $\alpha = 0°$ to $170°$ every $\Delta\alpha = 10°$. Although we could center our regions at any points in space we choose to center them on the coordinates of each atom i in the system.

Assuming a homogeneous applied shear stress, the local yield stress for the region surrounding atom i is defined as the minimum (positive) local shear stress threshold $\tau_i^c(\alpha)$ projected in the direction of remote loading α_l, i.e. for simple shear at orientation $\alpha_l = 0°$. We can express this as:

$$\tau_{y,i}(\alpha_l) = \min_{\alpha} \frac{\tau_i^c(\alpha)}{\cos(2(\alpha - \alpha_l))} \quad \text{with} \quad |\alpha - \alpha_l| < 45°. \quad (1)$$

We thus obtain microscopic information on the local yield stress for the amorphous structure to rearrange. Maps of local yield stress $\tau_{y,i}(\alpha_l = 0°)$ are exemplified in Fig. 1. It is apparent in Fig. 1c and 1d, where the first 10 events that occur during remote shear are denoted by open black symbols, that plastic events clearly tend to occur in regions characterized by low $\tau_{y,i}$.

Other local probes - Before proceeding to a more quantitative characterization of the correlation between the local yield stress and the development of the plastic activity, we note that other local properties have been proposed for the same purpose to which we can cross-compare our results. Here we consider the density ρ [42], the potential energy (PE) [10], the short-range order (SRO) [33, 43], the lowest shear modulus $2\mu^I$ [16] and the Participation Fraction (PF) as determined by an analysis of the quasi-localized soft vibrational modes [18]. These local properties can be divided between structural properties (ρ, PE, SRO) and linear responses ($2\mu^I$, PF). The structural properties are expected to reflect the local stability of the system and therefore, potentially, the susceptibility to mechanical loading. The main idea of linear response approaches is that the reversible rearrangements associated with low-energy deformation paths (computed perturbatively) will coincide with the irreversible plastic rearrangements.

For the sake of comparison, all of these local observables have also been computed [39]. The local structural properties are calculated for each atom from a coarse-graining process over a length scale $R_{GC} = 5\sigma$ [31, 44]. Local lowest shear moduli have been obtained following the method developed in Ref. [16]. The participation fraction of the low-energy vibrational mode has been computed following Ref. [18].

Correlation between plastic activity and local properties - To determine the reliability of local properties for predicting plastic activity one needs to quantify the relationship between the successive plastic event locations and the corresponding values of local properties computed from the configuration prior to the initiation of shear. In order to not introduce any arbitrary parameters when calculating this correlation, we work directly with the distribution of the different local properties. Plastic events are expected to occur in zones characterized by extremal values of the local estimators e.g. a minimum of the stress threshold $\tau_{y,i}$ or a maximum of the participation fraction PF_i. When the glass rearranges in a region centred on atom i, we thus compute the rank in the distribution of the local estimators at site i. The closer to the extremum, the higher the predictive quality of the local estimator. More precisely the correlation is defined based on the Cumulative Distribution Functions (CDF) value for a given local property at the location where the plastic event takes place (given by i_{max}). We define:

$$C_\psi = 1 - 2\overline{CDF}(\psi_{i_{max}}), \quad (2)$$

where ψ is one of the local properties and the average of its cumulative distribution functions $\overline{CDF}$ is performed over the different samples. C_ψ varies between -1 and 1 denoting perfect anti-correlation and perfect correlation, respectively. C_ψ will therefore be close to 1 when the plastic rearrangements are concentrated in zones where $CDF(\psi)$ is small. Note that Eq. (2) applies for a local property assumed to be relatively low at sites that exhibit plastic rearrangement, such as ρ, SRO, $2\mu^I$ and τ_y. Conversely, when the local indicator is supposed to increase with plastic susceptibility, the correlation is computed with the opposite of Eq. (2), as for PE and PF.

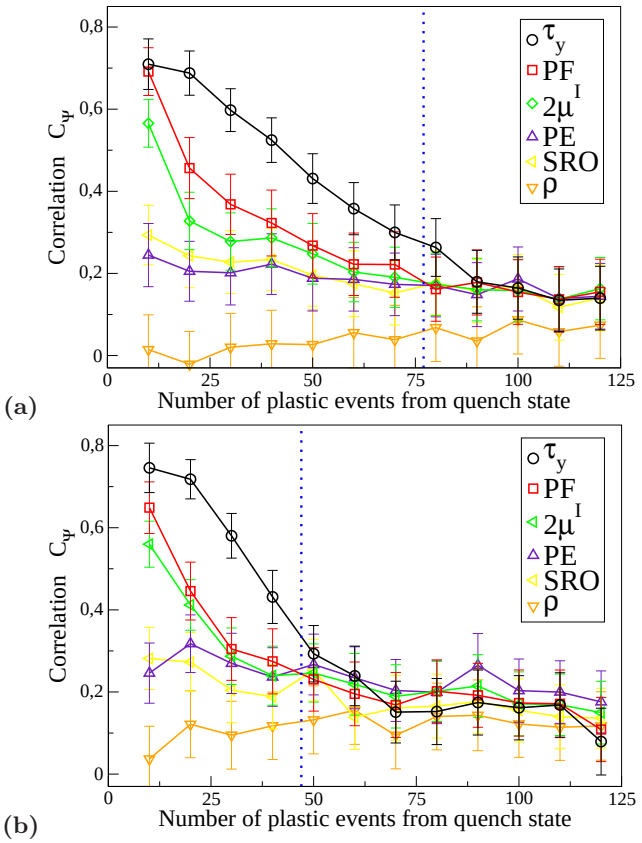

FIG. 2. Correlation between the local properties and the locations of the plastic rearrangement as a function of the number of plastic event from the quenched state for instantaneous (a) and gradual (b) quenches. The vertical line corresponds to $\gamma_{xy} = 0.07$.

This definition has the advantage of being consistent due to the direct use of the CDF and correlations can be directly compared with that which would be obtained from a random field, i.e. the worst scenario in terms of prediction.

Numerical results - The correlations calculated for all local properties are reported in Fig. 2 as a function of the number of events subsequent to the initiation of shear. Structural indicators (ρ, PE and SRO) show low-predictive power of the plastic activity. The only properties showing significantly high correlations are the minimum shear moduli, the participation fractions in low-frequency soft modes and the local yield stresses. The predictive power of the local yield stress calculations outperforms all other indicators. Most importantly, we see that its correlation C_{τ_y} persists even after many plastic rearrangements.

As expected, the correlations of $2\mu^I$, PF and τ_y decrease with the number of plastic events from the quenched state, as the material loses memory of its initial state during deformation. Surprisingly, we note that the correlations of PE and SRO are almost constant, with $C_\psi \approx 0.18$. Although small, this is higher than a white noise standard deviation (≈ 0.08). For most of the indicators, C_ψ converges toward the latter value. This suggests that while PE and SRO are not able to resolve individual zones, they may still be correlated with regions of high or low plastic activity on larger scales. Of course, at larger strain, we expect $C_\psi \to 0$ for all local properties.

The most striking results of this analysis is the slow decay of C_{τ_y}. For instance, considering the 25% of atoms having the smallest τ_y values (i.e. $C_{\tau_y} = 0.5$), it is possible to predict on average the locations of the first 43 (35) plastic events for the instantaneously (gradually) quenched system. The same reasoning applied to the linear response indicators shows that only the first 13 (14) and 18 (17) plastic event locations can be predicted for the instantaneously (gradually) quenched system considering the $2\mu^I$ and PF fields, respectively. For structural indicators, C_ψ simply never reaches a value equal to 0.5. C_{τ_y} starts to be comparable with the other local properties only from the 77th (43rd) plastic events for the instantaneously (gradually) quenched system, which corresponds to $\gamma_{xy} \approx 0.07$ as reported in Fig. 1a and 2.

Mechanical stability of glasses - The present method offers the opportunity to characterize the stability of the glass from a locally coarse-grained scale as a function of the quench protocol. Fig. 1a and 1b show a remarkable increase of the local yield stress with quench duration as the system achieves a greater degree of structural equilibration. The instantaneously quenched system is characterized by the presence of a multitude of small yield stresses. In contrast, these small thresholds are rarer in the more deeply quenched glass. We have calculated the yield stress distribution for both quench protocols as

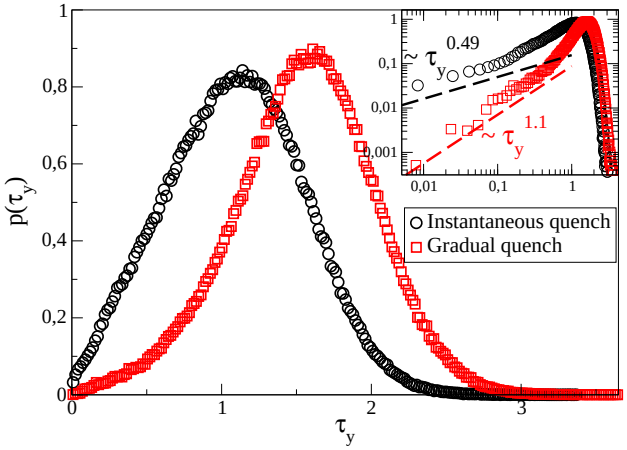

FIG. 3. Probability distribution function of the local yield stresses for instantaneous (circles) and gradual (squares) quenches. The same quantities are represented in log-scale in the inset. The straight lines (shifted for clarity) correspond to power law fits $\lim_{\tau_y \to 0} P(\tau_y) \sim \tau_y^\theta$ from which the tail exponents are estimated.

reported in Fig. 3. The general appearance of the distribution is qualitatively consistent with the energy barrier distributions found in [24, 45]. Local stress thresholds appear to be a very sensitive probe of the preparation of the glass and the plastic response. They are thus expected to be extremely useful for predicting the thermal history dependence of the plastic behavior in general and the shear-banding behavior in particular [10, 46].

We finally turn to the study of the tail of the stress threshold distributions in the limit of small thresholds. The latter is essential to determine how an STZs density might emerge in such a picture and how this could be used to model plasticity. Following [36, 47–50], we calculate the exponent θ characterizing the distribution $\lim_{\tau_y \to 0} P(\tau_y) \sim \tau_y^\theta$. We compute $\theta \approx 0.49$ for our instantaneously quenched glasses and $\theta \approx 1.1$ for our more gradually quenched glasses as reported in the insert of Fig. 3. These results are in qualitative agreement in the case of a system quenched instantly. For the slowly quenched system, our exponent deviates from the one found using an extreme value approach [48].

Conclusions - Our work sheds new light on the plasticity of amorphous materials by allowing a systematic characterization of the local yield stress thresholds from atomistic calculations. This nonperturbative local method provides an effective way to predict the location of plastic events even after large deformations. The correlation observed with low local yield stress outperforms other conventional structural indicators. Another advantage of our approach is that it gives access to the underlying distribution of stress thresholds and orientations. Quantifying the system in this way allows us to quantitatively distinguish material states of the system with different plastic susceptibility. A clear next step is

to find the minima in such a field to define and characterize the population of STZs in the amorphous solid. This is an essential and necessary step to transfer atomistically derived information to a larger scale and test the predictions of existing theoretical models as well as other emerging characterization methods[24–26, 51]. As such, this approach will allow a significant refinement of the multiscale modeling of mechanical properties of glassy systems.

M.L.F. acknowledges support from the U.S. National Science Foundation under Grant No. DMR 1408685 and both M.L.F. and S.P. under Grant No. DMR 1107838. Simulations were performed in part using The Maryland Advanced Research Computing Center (MARCC).

* sylvain.patinet@espci.fr

[1] D. Rodney, A. Tanguy, and D. Vandembroucq, Modelling Simul. Mater. Sci. Eng., **19**, 083001 (2011).
[2] A. Argon, Acta Metall., **27**, 47 (1979).
[3] M. L. Falk and J. S. Langer, Phys. Rev. E, **57**, 7192 (1998).
[4] D. L. Malandro and D. J. Lacks, J. Chem. Phys., **110**, 4593 (1999).
[5] C. E. Maloney and A. Lemaître, Phys. Rev. Lett., **93**, 016001 (2004).
[6] A. Tanguy, F. Leonforte, and J.-L. Barrat, Eur. Phys. J. E, **20**, 355 (2006).
[7] E. Lerner and I. Procaccia, Phys. Rev. E, **79**, 066109 (2009).
[8] J. Chattoraj and A. Lemaître, Phys. Rev. Lett., **111**, 066001 (2013).
[9] A. Lemaître, Phys. Rev. Lett., **113**, 245702 (2014).
[10] Y. Shi, M. Katz, H. Li, and M. Falk, Phys. Rev. Lett., **98**, 185505 (2007).
[11] M. L. Falk and J. S. Langer, Ann. Rev. Condens. Matter Phys., **2**, 353 (2011).
[12] E. Bouchbinder and J. S. Langer, Phys. Rev. E, **80**, 031133 (2009).
[13] V. V. Bulatov and A. S. Argon, Modell. Simul. Mater. Sci. Eng., **2**, 167 (1994).
[14] J.-C. Baret, D. Vandembroucq, and S. Roux, Phys. Rev. Lett., **89**, 195506 (2002).
[15] G. Picard, A. Ajdari, L. Bocquet, and F. Lequeux, Phys. Rev. E, **66**, 051501 (2002).
[16] M. Tsamados, A. Tanguy, C. Goldenberg, and J.-L. Barrat, Phys. Rev. E, **80**, 026112 (2009).
[17] R. L. Jack, A. J. Dunleavy, and C. P. Royall, Phys. Rev. Lett., **113**, 095703 (2014).
[18] J. Ding, S. Patinet, M. L. Falk, Y. Cheng, and E. Ma, Proc. Natl. Acad. Sci. U.S.A., **111**, 14052 (2014).
[19] A. Widmer-Cooper, H. Perry, P. Harrowell, and D. R. Reichman, Nat. Phys., **4**, 711 (2008); J. Chem. Phys., **131**, 194508 (2009); A. Ghosh, V. Chikkadi, P. Schall, and D. Bonn, Phys. Rev. Lett., **107**, 188303 (2011); K. Chen, M. L. Manning, P. J. Yunker, W. G. Ellenbroek, Z. Zhang, A. J. Liu, and A. G. Yodh, **107**, 108301 (2011).
[20] M. L. Manning and A. J. Liu, Phys. Rev. Lett., **107**, 108302 (2011).
[21] J. Rottler, S. S. Schoenholz, and A. J. Liu, Phys. Rev. E, **89**, 042304 (2014).
[22] M. Mosayebi, P. Ilg, A. Widmer-Cooper, and E. Del Gado, Phys. Rev. Lett., **112**, 105503 (2014).
[23] S. Schoenholz, A. Liu, R. Riggleman, and J. Rottler, Phys. Rev. X, **4**, 031014 (2014).
[24] D. Rodney and C. A. Schuh, Phys. Rev. Lett., **102**, 235503 (2009).
[25] Y. Fan, T. Iwashita, and T. Egami, Nat. Comm., **5**, 5083 (2014).
[26] Y. Fan, T. Iwashita, and T. Egami, Phys. Rev. Lett., **115** (2015).
[27] R. Dasgupta, S. Karmakar, and I. Procaccia, Phys. Rev. Lett., **108**, 134210 (2012).
[28] O. Gendelman, P. K. Jaiswal, I. Procaccia, B. Sen Gupta, and J. Zylberg, Europhys. Lett., **109**, 16002 (2015).
[29] S. Plimpton, J. Comp. Phys., **117**, 1 (1995).
[30] F. Lançon, L. Billard, and A. Chamberod, J. Phys. F: Met. Phys., **14**, 579 (1984).
[31] M. Widom, K. J. Strandburg, and R. H. Swendsen, Phys. Rev. Lett., **58**, 706 (1987).
[32] Y. Shi and M. L. Falk, Appl. Phys. Lett., **86**, 011914 (2005).
[33] Y. Shi and M. Falk, Phys. Rev. Lett., **95**, 095502 (2005).
[34] S. Nosé, J. Chem. Phys., **81**, 511.
[35] W. G. Hoover, Phys. Rev. A, **31**, 1695.
[36] S. Karmakar, E. Lerner, and I. Procaccia, Phys. Rev. E, **82**, 055103 (2010).
[37] C. E. Maloney and A. Lemaître, Phys. Rev. Lett., **93**, 195501 (2004).
[38] J. A. Zimmerman, D. J. Bammann, and H. Gao, Inter. J. Sol. Struct., **46**, 238 (2009).
[39] See Supplemental Material at (URL will be inserted by publisher) for comprehensive details on the numerical methods used to compute plastic event locations and the different local estimators.
[40] P. Sollich, in *CECAM Workshop* (ACAM, Dublin, Ireland, 2011).
[41] J. H. Irving and J. G. Kirkwood, **18**, 817 (1950).
[42] F. Spaepen, Acta Metall., **25**, 407 (1977).
[43] Y. Shi and M. L. Falk, Acta Mater., **55**, 4317 (2007).
[44] C. Goldenberg, A. Tanguy, and J.-L. Barrat, Europhys. Lett., **80**, 16003 (2007).
[45] D. Rodney and C. A. Schuh, Phys. Rev. B, **80**, 184203 (2009).
[46] D. Vandembroucq and S. Roux, Phys. Rev. B, **84**, 134210 (2011).
[47] J. Lin, A. Saade, E. Lerner, A. Rosso, and M. Wyart, Europhys. Lett., **105**, 26003 (2014).
[48] H. G. E. Hentschel, P. K. Jaiswal, I. Procaccia, and S. Sastry, Phys. Rev. E, **92**, 062302 (2015).
[49] J. Lin, T. Gueudré, A. Rosso, and M. Wyart, Phys. Rev. Lett., **115**, 168001 (2015).
[50] J. Lin and M. Wyart, Phys. Rev. X, **6**, 011005 (2016).
[51] E. Cubuk, S. Schoenholz, J. Rieser, B. Malone, J. Rottler, D. Durian, E. Kaxiras, and A. Liu, Phys. Rev. Lett., **114**, 108001 (2015).